A Circularly Polarized Antenna for UHF Satellite Communication Applications

K. Chitambara Rao [1, *], M. Lakshmunaidu [1], D. Nataraj [2], G. Vinutna Ujwala [3], and K. S. Chakradhar [4]

[1] Department of ECE, Aditya Institute of Technology and Management, Tekkali, Srikakulam, AP, India;
Email: laxman.naidu@gmail.com (M.L.)
[2] Department of ECE, Swarnandhra College of Engineering and Technology, Narsapur, West Godavari, AP, India;
Email: dasari.nataraj@gmail.com (D.N.)
[3] Department of ECE, Research scholar, Mohan Babu University, A. Rangampeta, Tirupati, AP, India;
Email: ujwala459@gmail.com (G.V.U.)
[4] Department of ECE, Mohan Babu University, Sree Sainath Nagar, A. Rangampeta, Tirupati, AP, India;
Email: chakradharec@gmail.com (K.S.C.)
*Correspondence: rao.chiddubabu@gmail.com (K.C.R.)

***Abstract*—There is a tremendous demand for antennas with very broad bandwidth and gain so that one antenna can cover the entire frequency range of the satellite communication applications, which are rapidly expanding with the current technology for diverse platforms. Helical antennas are ideal for these applications due to their distinctive qualities such as circular polarization, wide bandwidth, excellent gain, and low-profile conformability. For transmitting and receiving applications, which comprise frequency ranges of 240MHz to 270MHz and 290MHz to 320MHz, respectively. A new design of circularly polarized double-wire helical antenna employing the butterfly approach has been created in this study. An antenna was designed, simulated, analyzed, and fabricated before being experimentally measured for important parameters such as axial ratio, gain, 3dB beamwidth, and voltage standing wave ratio.**

***Keywords*—Single–wire helical antenna, double-wire helical antenna, butterfly technique, transformer feeding, ultra-high-frequency satellite communication**

I. Introduction

Since information and communication technologies connect cultures and groups, the modern world has grown dependent on them. Several industries, including emergency management, business continuity, the Internet of Things, oil and gas, government, healthcare, mining, maritime, logging, outdoor leisure, and more depend on satellite communications. Moreover, satellite communications are crucial for surveillance and security.

High-capacity applications have better Quality of Experience (QoE) when satellites are integrated with 5G infrastructure. Satellites preserve valuable spectrum by smartly routing and unloading traffic, increasing each network's resiliency. Despite being in its early stages of development, 5G shows promise for improving current problems. Satellite communication has been used for mobile networking as a stand-alone technology for many years. The satellites constructed utilizing 5G architecture are able to smoothly handle connectivity to vehicles, aircraft, and a variety of other devices in rural and remote places as this technology continues to progress. Satellite IoT (Internet of Things) services offered through satellite-based networks are referred to as IoT. IoT makes it possible for devices to be connected to one another so they may exchange information and convey commands without the need for human-to-human or even human-to-computer interaction. On the basis of the information obtained from remote devices, this enables the automation of thousands of decisions and activities. Conventional IoT devices connect to the internet through cellular networks, but cellular networks have significant limitations in terms of availability in rural areas.

A thorough overview of the most important methods, current solutions, difficulties, and prospects are provided along with a how-to manual for the modelling tools used in software defined satellite networks. An updated SDN-oriented approach is used in this survey to analyze the most recent developments of important approaches and solutions in software defined satellite networks. This survey provides an overview of current issues, fresh research possibilities, and publicly accessible simulation tools for generating further study [1]. A thorough analysis of recent developments and technical options in the design and creation of ground-breaking space-air-air networks has been done in order to allow seamless and widespread wireless connectivity for 6G wireless communications in the future. The paper begins with a thorough analysis of the space sector, concentrating on the classification of satellites, constellations, and present and potential developments in antenna technology. The air layer's significant significance in the delivery of next-generation services is next outlined and explored, followed by a thorough analysis of the topic. Also, the ground segment,

Manuscript received February 21, 2023; revised March 22, 2023; accepted April 3, 2023.

doi:10.12720/jcm.18.10.643-657

which focuses on both user terminals and the gateway antenna, receives special attention. Finally, pertinent application scenarios for the Space-Air-Ground Integrated Network (SAGIN) paradigm in current and future wireless communications are covered, including use cases for 5G, B5G, and 6G [2]. The capacity of phased array antennas to produce a variety of beams by the beamforming network and support numerous satellites at once makes them excellent candidates to meet the needs of routine management and control operation of a future ultra-dense LEO satellite constellation. Phased array antennas for satellite ground stations have a number of benefits over conventional reflector antennas, including better performance, greater dependability, and reduced cost [3]. A microstrip patch antenna was made for CubeSat applications in the UHF band. This antenna achieves an axial ratio of less than 3 dB, a gain of 5.82dBi, and a reflection coefficient of -10dB [4]. Many antenna designs, including helical antennas, patch antennas, dipole and monopole antennas, reflector antennas, slot antennas, reflector array antennas, millimetre and sub-millimeter wave antennas, and meta surface antennas for Cube Satellites, had been evaluated. The various antennas have also been divided into categories according on the frequency bands, including VHF, UHF, L, S, C, X, Ku, and K/Ka. Also, all of the antennas' characteristics, including their gain, bandwidth, and reflection coefficient, were compared [5]. On a double-layer ceramic substrate, two monopole antennas were merged to form a single antenna that is suggested for CubeSat applications at two frequencies, such as 149 MHz (VHF) and 398 MHz (UHF). The antenna is 101 mm by 40 mm by 8.9 mm. With the aid of a foldable structure and the meander-line approach, a small design for this antenna has been made possible. With this antenna, you may increase gain, improve matching, and reduce coupling [6]. For the 1U BIRDS-1 CubeSat, a small patch antenna with a coaxial-fed method was introduced at a UHF frequency of 437.375MHz on one side of the substrate, a partial ground plane and a spiral meander line patch were employed to create this antenna. The suggested antenna was created using a 1.57-mm-thick single-layer Roger's substrate with a relative permittivity of 2.2 and has dimensions of $0.105\lambda \times 0.047\lambda \times 0.002\lambda$ at 437.375MHz [7]. The quadrifilar helix antenna and the conical log spiral antenna were presented as two different types of antennas for CubeSats operating in the UHF band. S2 glass fiber-reinforced epoxy and beryllium copper were used to create the quadrifilar helix antenna. Composite materials like phosphor bronze and fiber were used to create a conical log spiral antenna. Both of these two antennas were built, their performance was evaluated, and CubeSat deployment options were researched [8]. For VHF and UHF SATCOM applications at the frequencies of 295 MHz and 355 MHz, a unique miniaturized four-element sequential-rotation array antenna was described. The size of the constructed antenna, $0.197\lambda \times 0.197\lambda \times 0.068\lambda$, was measured along with the axial ratio, gain, and reflection coefficient. A gain of 4.5dBi, a reflection coefficient of -9.5 dB, and an axial ratio of 1.15 dB were measured for this antenna [9]. For the downlink and uplink frequencies of 146MHz and 438MHz, respectively, a dual-band spring-steel monopole antenna was created. To separate the transmitting and receiving frequencies for this antenna, a diplexer has been used [10]. For using in satellite communication applications at a frequency of 1.575GHz, a circularly polarized antenna was suggested. The suggested antenna is composed of two components, such as phase-fed folded monopoles and sequentially fed L-shaped monopoles. The omnidirectional circular polarized radiation pattern is produced by phase-fed folded monopoles, whereas the broadside circular polarized radiation pattern is produced by sequential-fed L-shaped monopoles. For left-handed circular polarization with upper hemisphere coverage, these two components are merged and used as a pattern diversity antenna. In the frequency range between 1.515 GHz and 1.62GHz, the suggested antenna achieves a -10 dB impedance bandwidth and a 3 dB axial ratio of 6.7% [11]. For using with low-Earth orbit (LEO) satellite applications, a quadrifilar helix antenna in the UHF band was created. Based on a straightforward impedance matching network, this antenna has been optimized [12]. Based on the U-slots, a circularly polarized stacking patch antenna was created and put out for using in UHF satellite communication applications in the 240 MHz to 300 MHz frequency range. The proposed antenna measures $0.36\lambda c \times 0.36\lambda c \times 0.035\lambda c$ in size and achieves a 22% bandwidth, 3.5dBi of gain, and an axial ratio under 2.5 dB [13]. Based on a thin ferrite ground plane, a spiral antenna was created for lower earth orbit satellite applications in the UHF band, such as 243MHz to 318MHz.The gain of this antenna is more than 0dBi, and its Voltage Standing Wave Ratio (VSWR) is 2:1 [14]. The design equations for a double-wire helical antenna have been published by John D. Kraus and are appropriate for satellite communication applications [15]. Due to its ease of fabrication, compact size, and great efficiency, a double-wire helical antenna was shown to be suitable for satellite communication applications [16]. A minimum gain of 0dBi is required for successful communication between the earth station and satellite, according to Timothy Pratt's gain calculations for satellite communication applications [17]. To achieve good radiation characteristics, including impedance matching, axial ratio, bandwidth, and gain, a variety of approaches, including flared open ends, tapered feed ends, and the FDTD algorithm, are applied [18–22]. An array of two double-wire helical antennas was utilized in the AMS and TMI systems to eliminate the direction of beam movement [23]. A new reconfigurable double-wire helical antenna was made by changing the wires' heights [24].

The design of many types of antennas, including patch antennas, spiral antennas, and quadrafilar helical antennas, for using in UHF and VHF satellite communication applications is described in the available literature. In this study, a brand-new design idea for a bifilar or double-wire helical antenna with a butterfly approach is put forth. The performance of the proposed antenna has been improved when compared to other helical antennas in the open literature by using the butterfly technique. Furthermore, the performance of the four significant parameters, such as

VSWR, gain, axial ratio, and 3dB beamwidth, has been improved, and the practical frequencies of UHF satellite communication applications have been verified using the proposed antenna.

This work is organized into six sections. Section I offers a brief introduction to the subject and provides the crucial literature review. Section II provides how the antenna design is made in the simulation software with the help of initial dimensions and design parameters. Section III provides the simulation results, which show the various antenna parameters like Voltage Standing Wave Ratio (VSWR), Axial ratio, 3 dB beam width, and gain. Apart from this, all these parameters are analyzed to determine the performance of the designed antenna. Section IV provides the fabrication and measurement results. In this section, the fabrication of an antenna is discussed. Apart from this, the fabricated antenna has been measured for various characteristics like Voltage Standing Wave Ratio (VSWR), Axial ratio, 3 dB beam width, and gain, and these parameters are also analyzed to determine the performance of an antenna. Section V provides the results and discussion in terms of the comparison of simulated and measured results to obtain the validation of an antenna for use in ultra-high-frequency (UHF) satellite communication applications. Section VI provides the conclusion of the proposed work.

II. Antenna Design

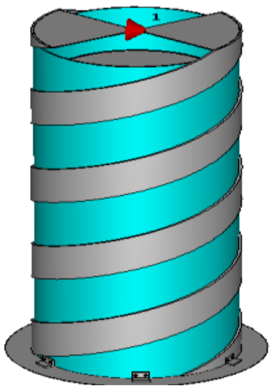

Figure 1. Double-wire helical antenna.

The characteristics of the electromagnetic waves that travel along such a helical structure can be used to comprehend how the bifilar or double-wire helix operates as an antenna. A fast reverse wave can be supported with the right choice of helical parameters. This kind of wave has a phase velocity larger than the speed of light and will radiate easily as a result. The group velocity, which represents the flow of energy, is, slower than the speed of light and moves in the opposite direction from the phase velocity. The currents on the wires are equal in amplitude but run in the opposite direction, and the wave of interest on the bifilar or double-wire helix is balanced. It is possible to create a unique aerial for satellite communication applications by utilizing these fundamental features. Think of a straightforward helix made up of just one wire, like a typical spring. A unifilar helix is another name for this arrangement. A bifilar helix structure, also known as a double-wire helix, is created when two of these springs are intermeshed with their center lines aligned. The most common geometry is symmetrical. A spring is 180^0 turns apart from another spring. A quadrifilar helix is produced by expanding this idea to four springs with 90^0 spaces between the individual components. A coaxial transmission line, which has equal and opposing currents running on its inner and outer conductors, is typically used to feed the helix of an antenna. Typically, a unifilar helix is attached to the coaxial cables center conductor, where the current flowing through it is equal to the current flowing through the inner conductor. A ground plane that is electrically coupled to the outer conductor receives the opposite current flowing radially from that conductor. As a result, it is frequently said that the unifilar helix is "fed against a ground plane." Contrarily, no ground plane is necessary to excite a bifilar helix or dual wire helix because equal and opposing currents are applied to the two wires. The frequency range of 240 MHz to 320 MHz has been designed for a double-wire helical antenna (see Fig. 1). A double-wire helical antenna's two wires are linked at the end in the form of a butterfly. It is believed that a butterfly arc can be as long as $\lambda/4$. The butterfly arc length and spacing between the coils are tuned to obtain the best axial ratio and gain values based on the specified helix diameter and number of turns. For impedance matching between the antenna and free space, the feeding connection is made at the junction of two wires. In order to create left-hand circular polarization (LHCP) for this antenna, the two helix wires on the cylinder are wound anticlockwise. The two helix wires on the cylinder can alternatively be twisted in a clockwise orientation to produce right-hand circular polarization (RHCP). Depending on the application, LHCP or RHCP may also be utilized for satellite communication. According to the link budget estimates for satellite communication, the needed gain values for the earth station and satellite are -3dBi and +3dBi, respectively, for successful communication. This antenna is intended for many platform applications, hence, the ground plane may or may not be employed. The platform surface will serve as the ground plane in applications such as ships and submarines where the ground plane is not necessary. Thus, a ground plane is not required in the design of a double-wire helical antenna. Furthermore, hemispheric coverage is taken into consideration as this antenna is made for UHF satellite communication applications. The two opposing wires of a double-wire helical antenna are fed at one end by balanced currents. There is an 1800 phase shift between those wires. A new kind of circularly polarized antenna is obtained when two opposing wires of a double-wire helical antenna are fed at one end by balanced currents by providing an 1800 phase shift between those wires. By balancing the current distributions in both of the helical antenna's arms, circular polarization can be obtained in a double-wire helical antenna. The double-wire helical antenna generates a beam that is directed along the structure in the direction of the feed point when it is operated above the cut-off frequency of the principal mode of the helical waveguide.

A. Design Equations

$$\text{Antenna gain (G)} = 10.8 + 10\, log\left[\left(\frac{C}{\lambda}\right)^2 \; N\frac{S}{\lambda}\right] \quad (1)$$

$$\text{Circumference (C)} = \text{Wavelength } (\lambda) \quad (2)$$

$$\text{Diameter (D)} = \frac{C}{\pi} \quad (3)$$

$$\text{Antenna height (H)} = NS \quad (4)$$

$$Tan\alpha = \left(\frac{S}{C}\right) = \frac{S}{\pi D} \text{ or } \alpha = \text{Tan}^{-1}\left(\frac{S}{\pi D}\right) \quad (5)$$

$$\text{Ground plane diameter } (G_d) = \frac{3\lambda}{4} \quad (6)$$

$$\text{Butterfly arc length (Bal)} = \frac{\lambda}{4} \quad (7)$$

$$\text{Butterfly side length } (B_{sl}) = \frac{D}{2} \quad (8)$$

B. Design Specifications and Parameters

Table I leads to the conclusion that an antenna's characteristics are taken into account in light of earlier research [3]. The design equations, which are described in Section II.A, are also used to compute the design parameters.

TABLE I. DESIGN SPECIFICATIONS AND PARAMETERS OF DOUBLE-WIRE HELICAL ANTENNA

S.NO	Design Parameter	Specification	Parameter	Calculated value
1	Receiving frequency range	240MHz-270MHz	Centre frequency	280MHz
2	Transmitting frequency range	290MHz-320MHz	Wavelength(λ)	1070mm
3	VSWR	3:1(Max.)	Number of turns(N)	2.5
4	Gain	-3dBi (Min) to 3dBi (Max)	Spacing between coils(S)	357mm
5	Polarization	LHCP	Diameter(D)	340mm
6	Beam width	± 45° from vertical 90^0(max) &17.03^0(min)	Antenna height(H)	893mm
7	Axial Ratio	<5dB	Pitch angle((α)	18.36^0
8	Spatial coverage	Over top hemisphere	Ground plane diameter (G_d)	802mm
9	Input impedance	50 Ω	Butterfly arc&side lengths (B_{al} & B_{sl})	267mm&170mm
10	Connector	SMA	Helix wire width(d)	12mm

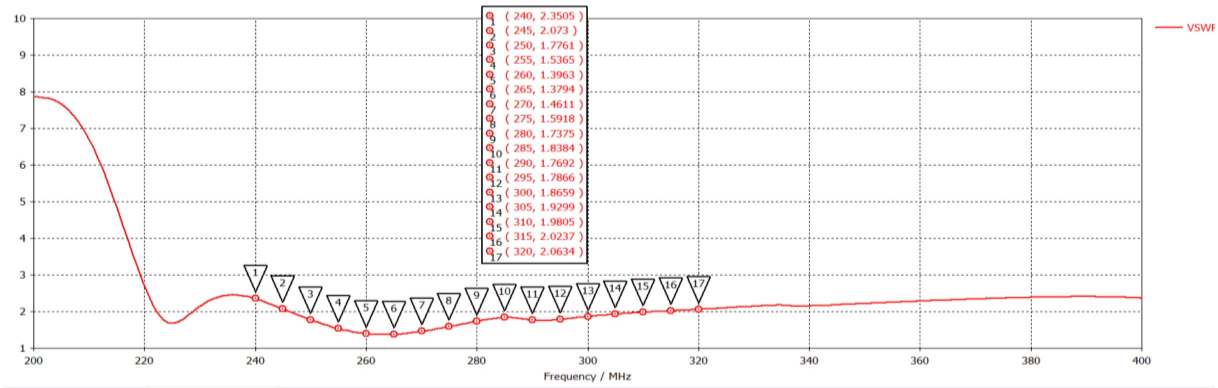

Figure 2. VSWR versus frequency.

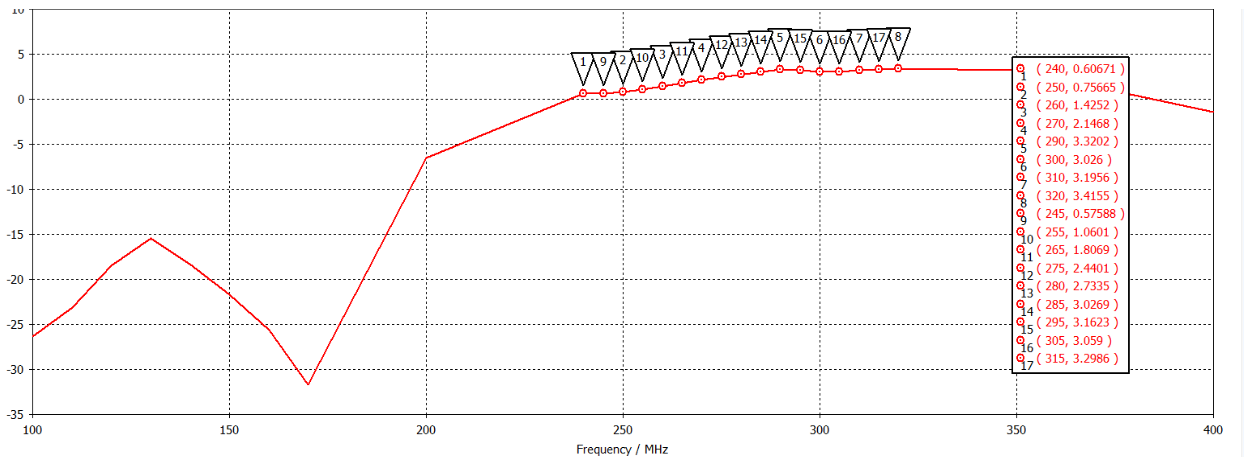

Figure 3. Gain versus frequency at θ= -45^0.

III. SIMULATION RESULTS

Based on design parameters, a butterfly helical antenna is simulated and examined for its many properties at various resonant (receiving and transmitting) UHF satellite communication frequencies, including VSWR, gain, axial ratio, 3dB beam width, and radiation patterns. In order to perform further analysis, the "φ" is set to 0^0 to measure the antenna's gain and axial ratio at two distinct angles (-45^0, 0^0 and 45^0). For examination, the radiation pattern properties, radiation patterns like 3D and 2D are also captured at various resonant frequencies.

A. VSWR

VSWR is plotted against frequency in Fig. 2. The X-axis is used to measure frequency, and the Y-axis is used to measure VSWR. The VSWR curve reveals that the VSWR is essentially constant throughout the UHF satellite communication band. In addition to this, the uplink frequencies have a higher value of VSWR than the downlink frequencies.

B. Gain

Figs. 3 to 5 show the frequency versus gain for various angles of θ (-45^0, 0^0, and 45^0).

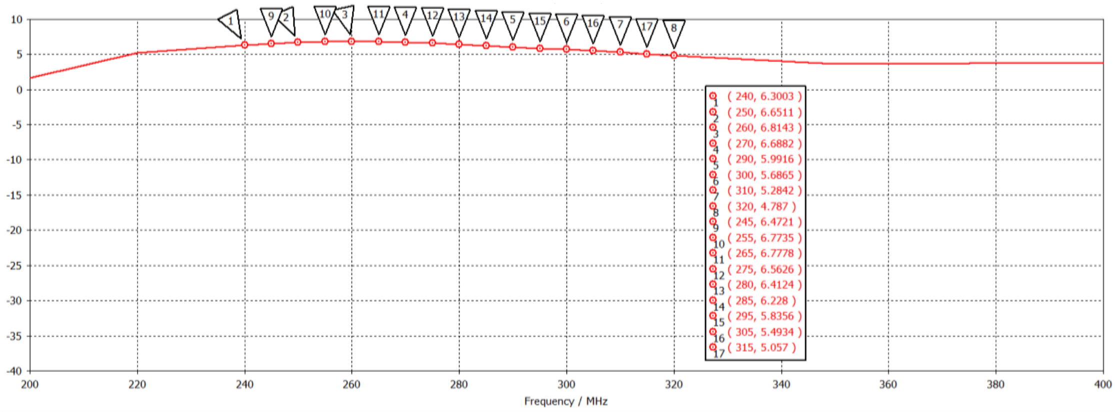

Figure 4. Gain versus frequency at $\theta=0^0$.

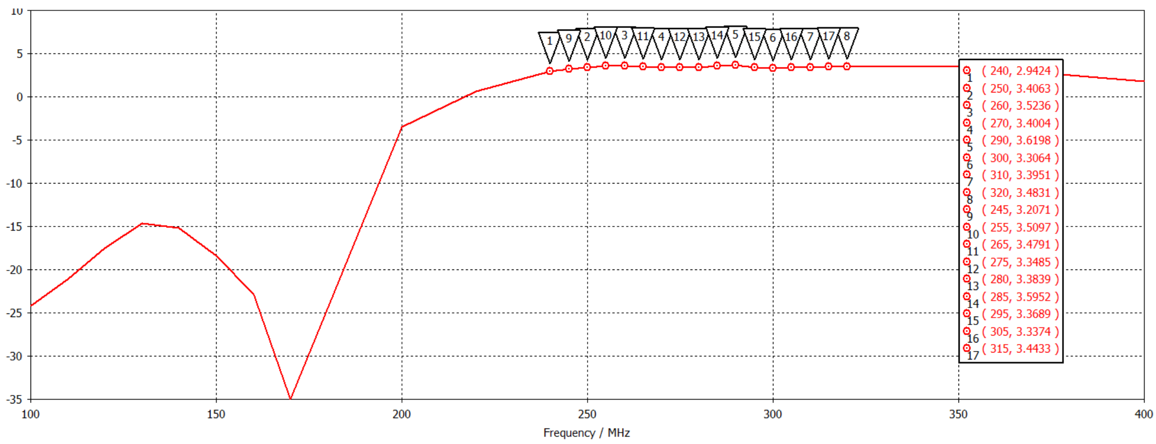

Figure 5. Gain versus frequency at $\theta=45^0$.

TABLE II. VSWR AND GAIN AT DIFFERENT ANGLES OF Θ FOR VARIOUS RESONANT FREQUENCIES

Freq (MHz)	VSWR	Simulated Gain(dBi)		
		-45^0	0^0	45^0
240	2.3505	0.6067	6.3003	2.9474
250	1.7761	0.7566	6.6511	3.4063
260	1.3963	1.4252	6.8143	3.5236
270	1.4611	2.1468	6.6882	3.4004
280	1.7375	2.7335	6.4124	3.3839
290	1.7692	3.3202	5.9916	3.6198
300	1.8659	3.026	5.6865	3.3064
310	1.9805	3.1956	5.2842	3.3951
320	2.0634	3.4155	4.787	3.4831

The values for the simulated VSWR in Table II were taken from Fig. 2. According to Table II, the lower VSWR values at the resonant frequencies are 1.3963 at 260MHz and 1.7692 at 290MHz, respectively. The best and most appropriate VSWR values for UHF satellite communication applications are those with lower values.

Gain vs frequency at several angles of (-45^0, 0^0, and 45^0) are shown in Figs. 3–5. Gain is measured along the Y-axis, and frequency is measured along the X-axis. Table II displays the simulated gain from Figs. 3 to 5 at various angles. The largest gain values, when compared to -45° and +45°, are obtained at $\theta = 0^0$, as can be seen from Table II. Also, it is noted that the higher gain values at 0° for the resonant frequencies are 6.8143dBi at 260MHz and 5.9916dBi at 290MHz, respectively. The higher gain values are 2.1468 dBi at 270MHz, 3.4155 dBi at 320 MHz, 3.5236 dBi at 260MHz, and 3.6198 dBi at 290MHz, respectively, at -45° and +45°. According to the provided design criteria, these higher gain values are good and suitable for UHF satellite communication applications.

C. Axial Ratio

Figs. 6 to 8 show the frequency versus axial ratio for various angles of θ (-45^0, 0^0, and 45^0).

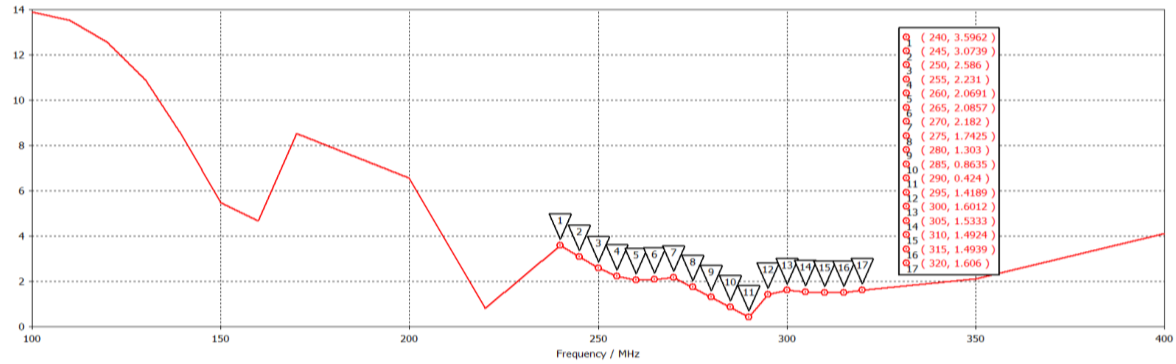

Figure 6. Axial ratio versus frequency at θ= -45^0.

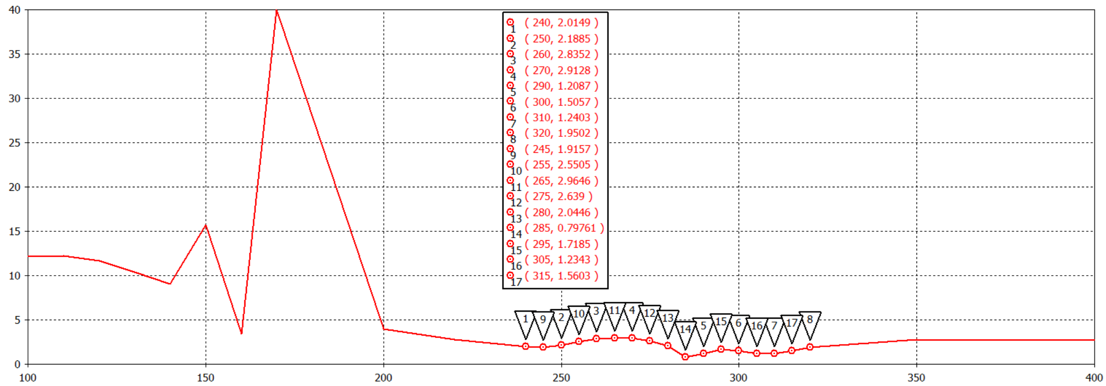

Figure 7. Axial ratio versus frequency at θ= 0^0.

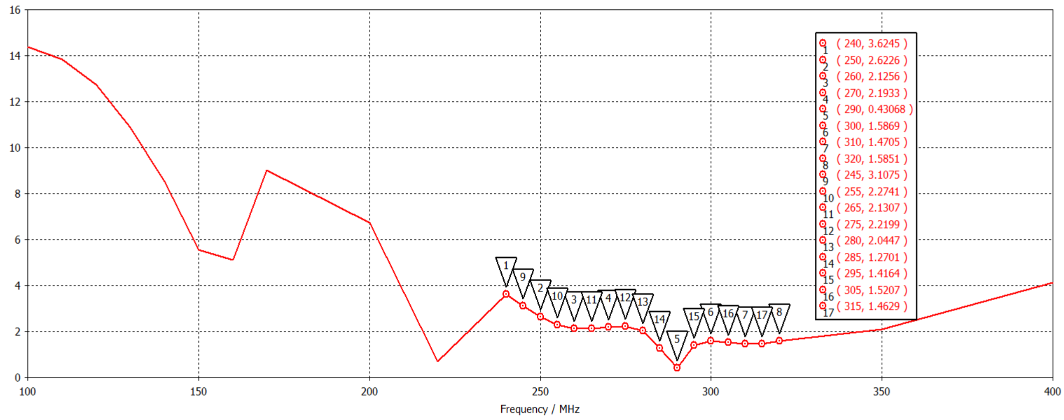

Figure 8. Axial ratio versus frequency at θ= 45^0.

D. Radiation Patterns at Various Receiving and Transmitting Frequencies

Since it is highly challenging to evaluate 3D radiation patterns, 2D radiation patterns must be used instead to determine the properties of the radiation pattern. Additionally, by changing the ‘θ’ for the fixed value of ‘φ’ at 0^0. 2D radiation patterns are deduced from 3D radiation patterns.

Figs. 6 to 8 display the relationship between axial ratio and frequency for various values of (-45°, 0^0, and 45°). On the X-axis, frequency is measured, and on the Y-axis, axial ratio. The simulated axial ratio from Figs. 6 to 8 is given in Table III at various angles. The lower axial ratio values at 0^0 for the resonant frequencies are 2.0149dB at 240 MHz and 1.2087dB at 290MHz, respectively, according to Table III. The lower axial ratio values are similarly 2.0691 dB at 260MHz, 0.4189dB at 290MHz, 2.1256dB at 260 MHz, and 0.43068dB at 290MHz at -45° and +45°, respectively. According to the provided design criteria, these reduced axial ratio values are good and suitable for UHF satellite communication applications. Simulated 3D and 2D radiation patterns at different resonance frequencies are shown in the Figs. 9–17. The 3dB simulated beam width values in Table III were calculated from the 2D radiation patterns. Table III shows that at the resonant frequencies, the greater 3dB beam width values are 95.3^0 MHz at 270MHz and 114.9^0 at 320MHz, respectively. For UHF satellite communication applications, these greater 3dB beam width values are desirable and appropriate.

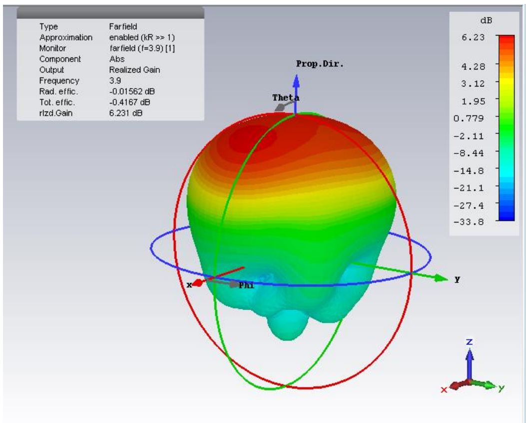

(a)3D Pattern

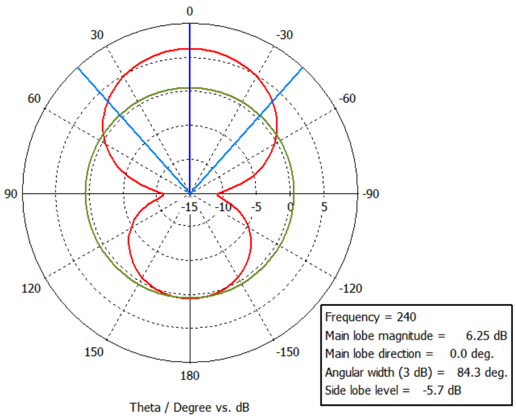

(b) 2D Pattern

Figure 9. Radiation patterns at 240MHz.

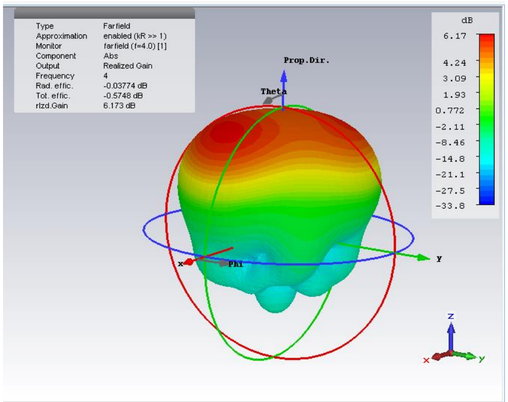

(a)3D Pattern

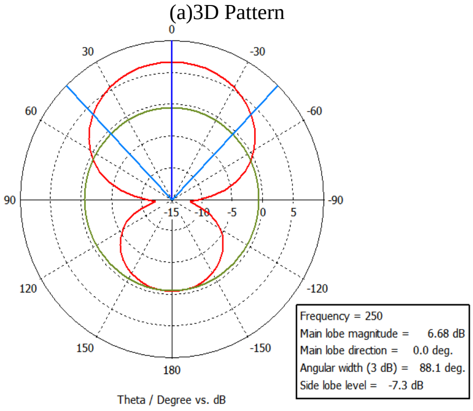

(b) 2D Pattern

Figure 10. Radiation patterns at 250MHz

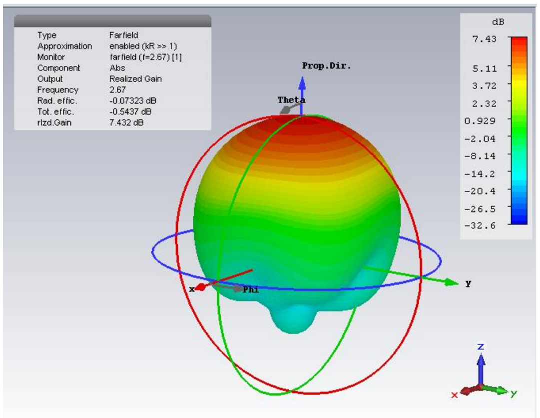

(a)3D Pattern

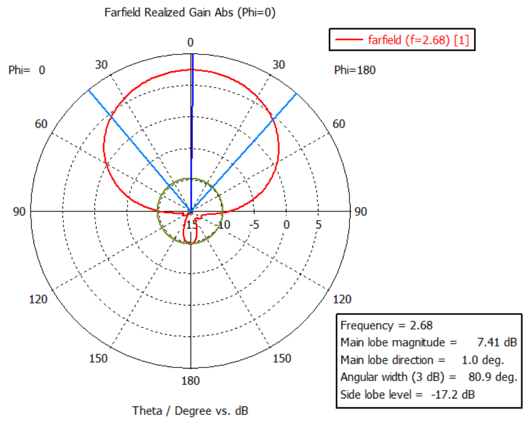

(b) 2D Pattern

Figure 11. Radiation patterns at 2.68MHz.

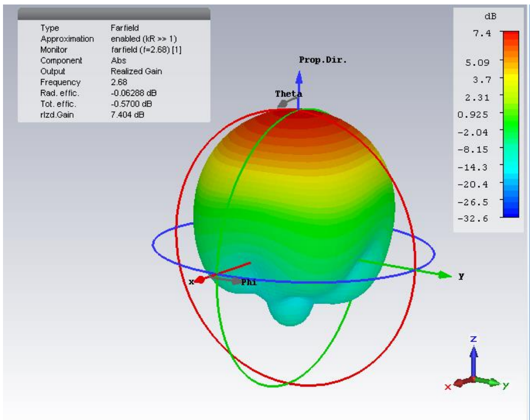

(a)3D Pattern

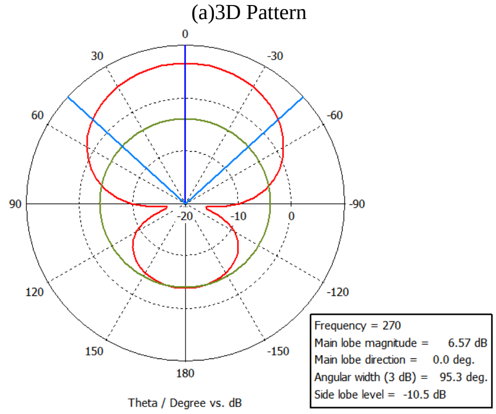

(b) 2D Pattern

Figure 12. Radiation patterns at 270MHz.

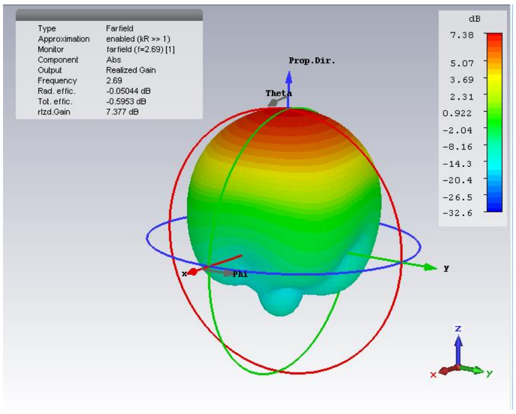

(a)3D Pattern

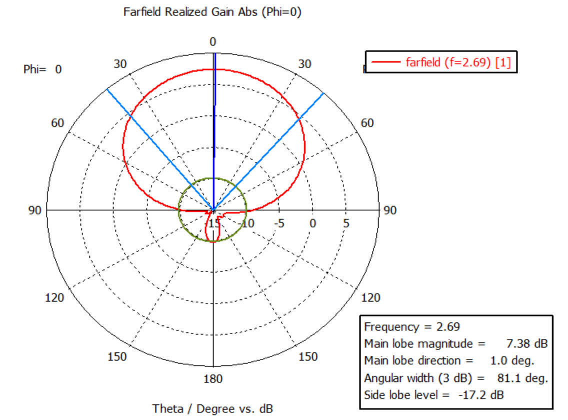

(b) 2D Pattern

Figure 13. Radiation patterns at 2.69MHz.

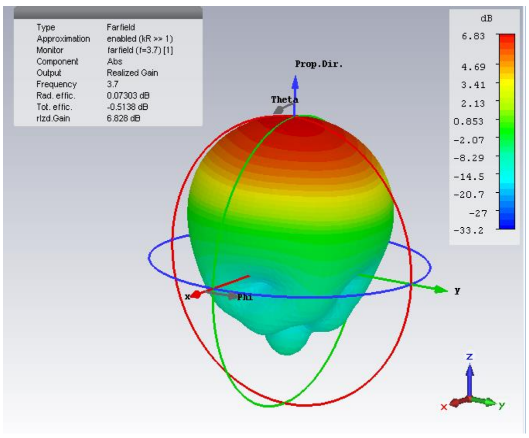

(a)3D Pattern

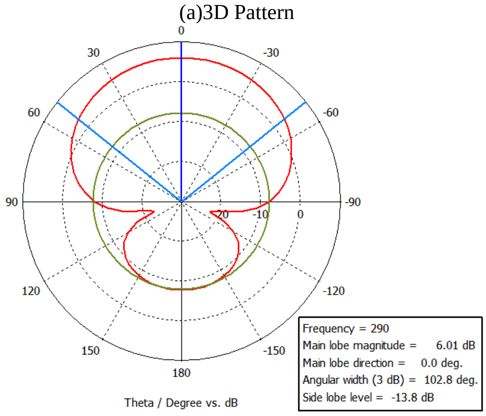

(b) 2D Pattern

Figure 14. Radiation patterns at 290MHz.

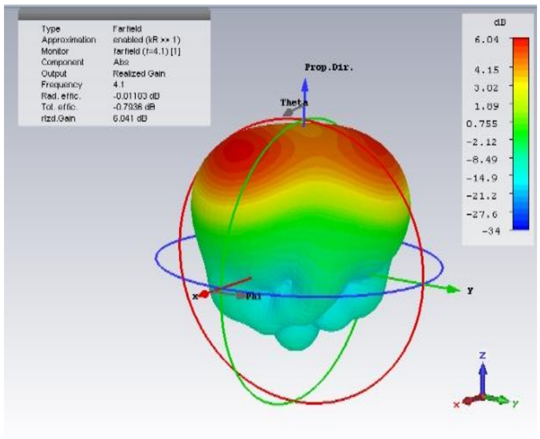

(a)3D Pattern

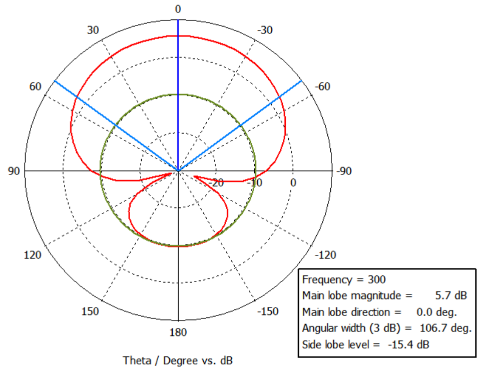

(b) 2D Pattern

Figure 15. Radiation patterns at 300MHz.

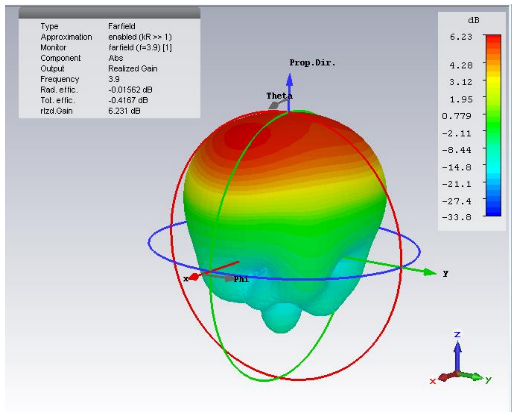

(a)3D Pattern

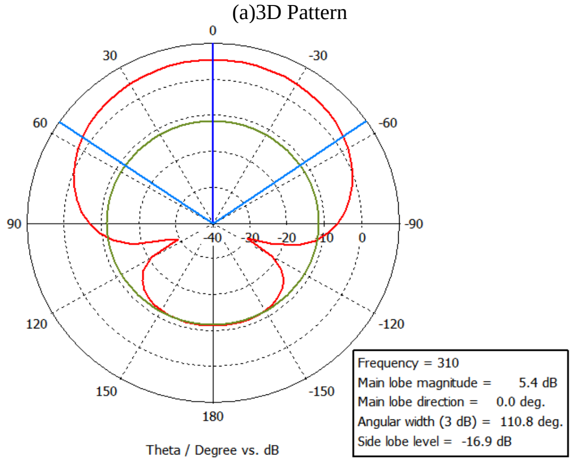

(b) 2D Pattern

Figure 16. Radiation patterns at 310MHz.

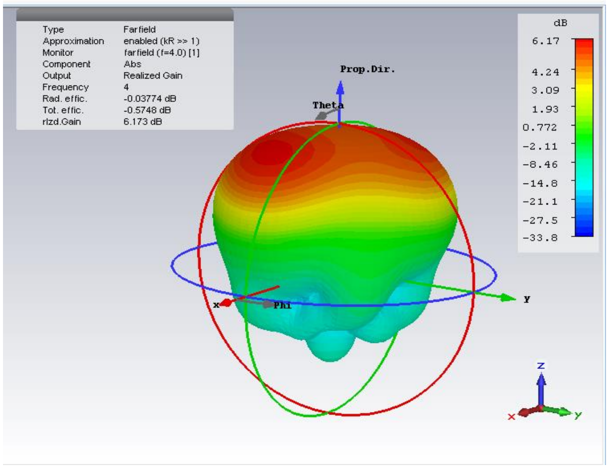

(a)3D Pattern

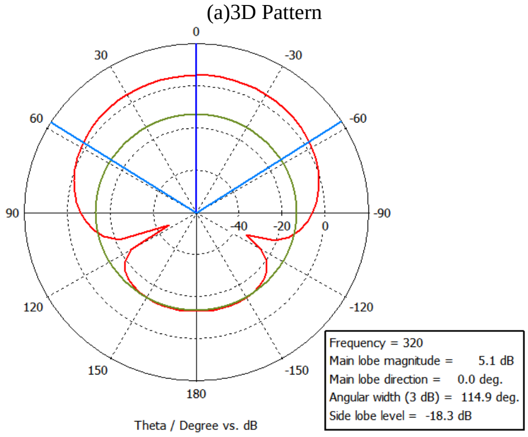

(b) 2D Pattern

Figure 17. Radiation patterns at 320MHz.

TABLE III. SIMULATED 3DB BEAM WIDTH AND AXIAL RATIO AT VARIOUS RESONANT FREQUENCIES

Frequency (MHz)	3dB beamwidth	Simulated axial ratio		
		- 45^0	- 45^0	- 45^0
240	84.3	3.5962	3.5962	3.5962
250	88.1	2.586	2.586	2.586
260	91.8	2.0691	2.0691	2.0691
270	95.3	2.182	2.182	2.182
280	89.7	1.303	1.303	1.303
290	102.8	0.4189	0.4189	0.4189
300	106.7	1.6012	1.6012	1.6012
310	110.8	1.4924	1.4924	1.4924
320	114.9	1.606	1.606	1.606

IV. FABRICATION AND MEASUREMENT RESULTS

Fig. 18 shows the fabricated double-wire helical antenna. Based on design parameters, the double-wire helical antenna is fabricated. Copper material is used for helix wire. The helix wire is fed by a normal transformer, which matches the antenna impedance 50Ω to free space impedance 377Ω. The fabricated antenna has been measured for the various characteristics such as VSWR, Gain, 3-dB beam width, axial ratio and radiation patterns in horizontal and vertical polarizations for various receiving and transmitting frequencies.

Figure 18. Fabricated double-wire helical antenna.

A. *Measured VSWR*

The link between VSWR and frequency is seen in Fig. 19. The X-axis is used to measure frequency, and the Y-axis is used to measure VSWR.

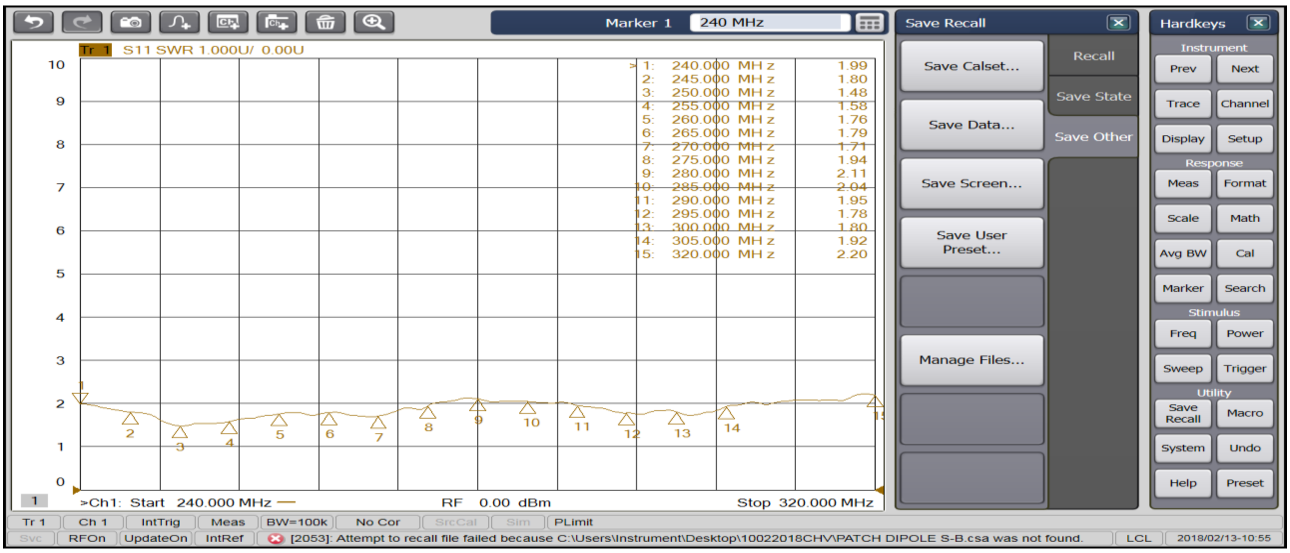

Figure 19. Measured VSWR versus frequency.

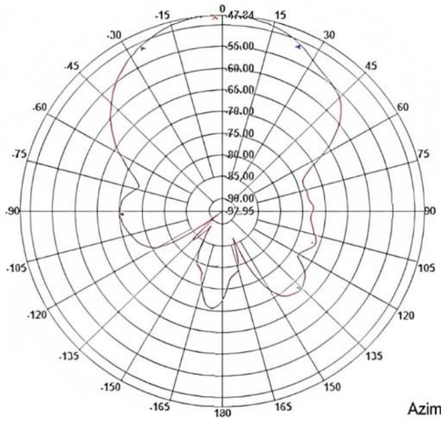

Figure 20. Radiation pattern at 240MHz.

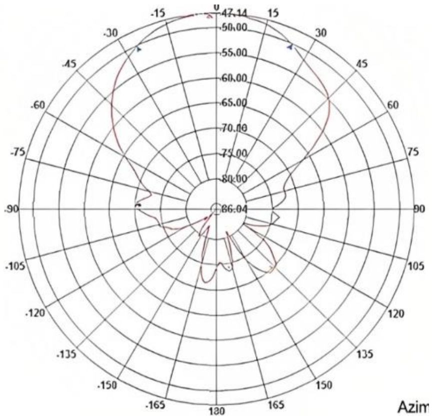

Figure 21. Radiation pattern at 250MHz.

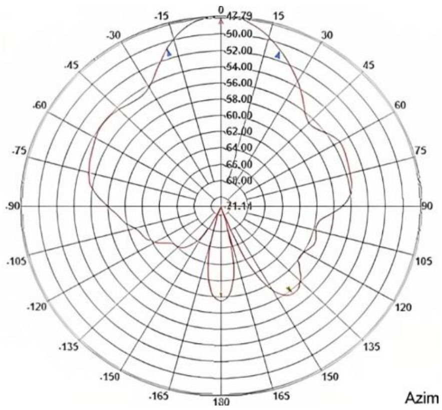

Figure 22. Radiation pattern at 260MHz.

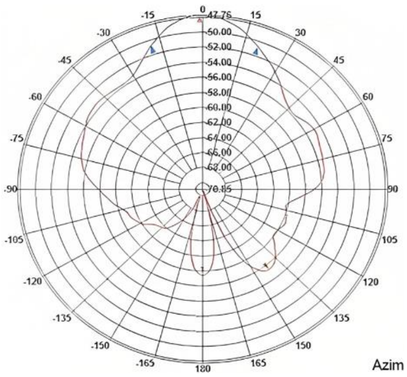

Figure 23. Radiation pattern at 270MHz.

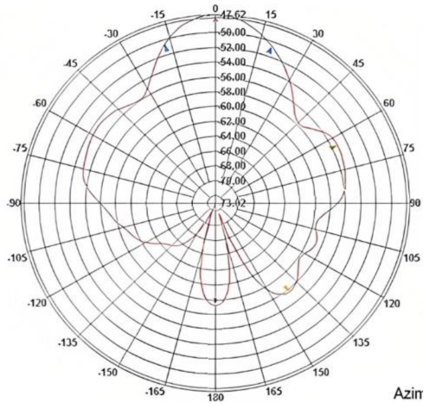

Figure 24. Radiation pattern at 280MHz.

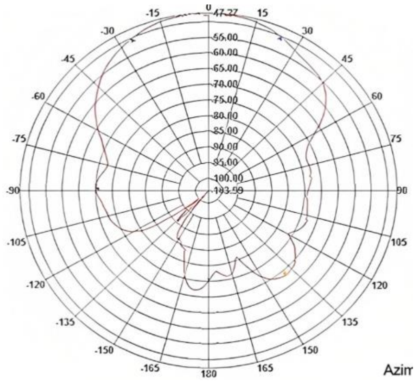

Figure 25. Radiation pattern at 290MHz.

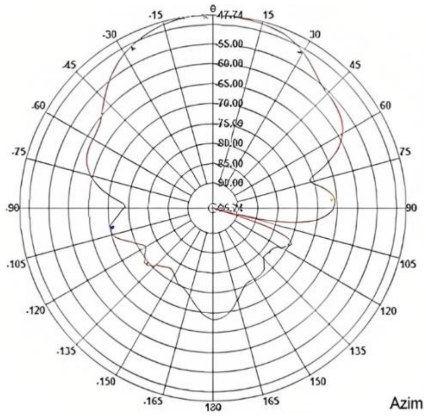

Figure 26. Radiation pattern at 300MHz.

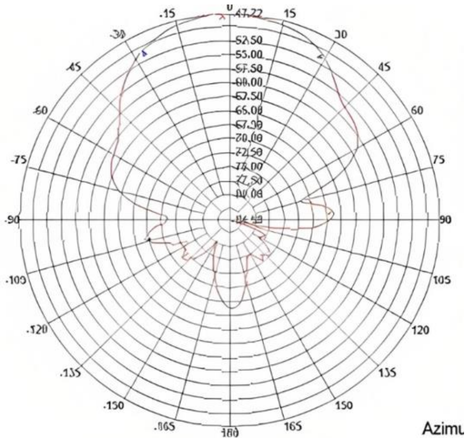

Figure 27. Radiation pattern at 310MHz.

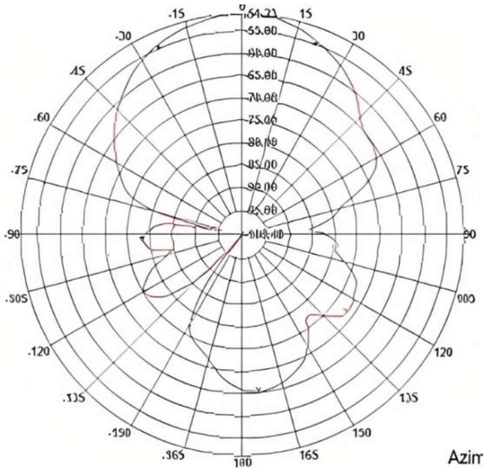

Figure 28. Radiation pattern at 320MHz.

B. Measured Radiation Patterns in Horizontal Polarization(HP) at Various Receiving and Transmitting Frequencies

Figs. 20 to 28 show the measured radiation patterns of fabricated antenna in horizontal polarization at various receiving and transmitting frequencies. To get a measurement of radiation pattern of designed antenna or antenna under test in horizontal polarization, a designed antenna or antenna under test is put down at the receiving side in a horizontal position, and the normal horn antenna (1GHz–18GHz) is put down at the transmitting side in a horizontal position. After placing them properly, note down the power values of the designed antenna using antenna software.

C. Measured Radiation Patterns in Vertical Polarization(VP) at Various Receiving and Transmitting Frequencies

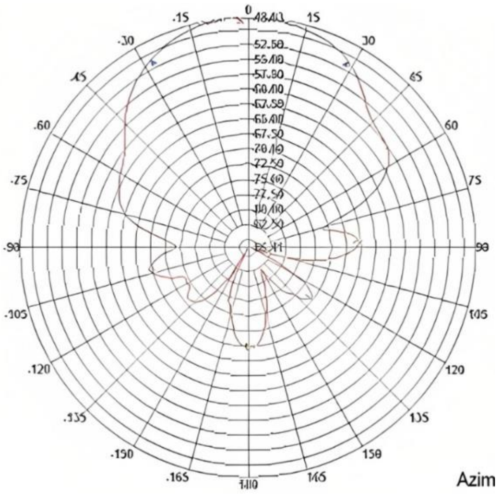

Figure 29. Radiation pattern at 240MHz.

Figs. 29 to 37 show the measured radiation patterns of fabricated antenna in vertical polarization at various transmitting and receiving frequencies. To get a measurement of radiation pattern of designed antenna or antenna under test in vertical polarization, a designed antenna or antenna under test is put down at the receiving side in a vertical position, and the normal horn antenna (1GHz–18GHz) is put down at the transmitting side in a vertical position. After placing them properly, note down the power values of the designed antenna using antenna software.

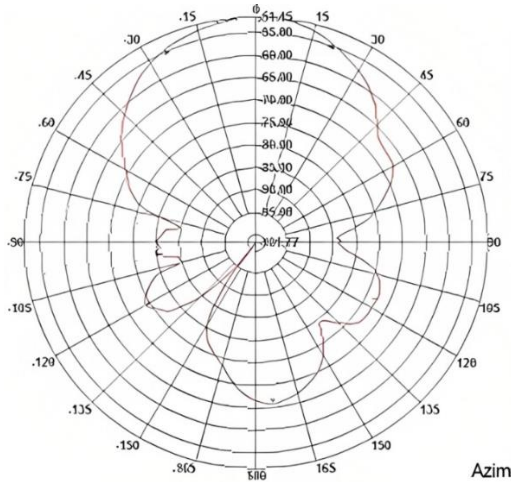

Figure 30. Radiation pattern at 250MHz

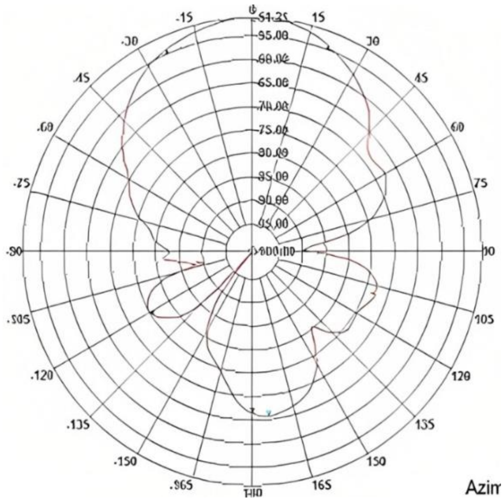

Figure 31. Radiation pattern at 260MHz.

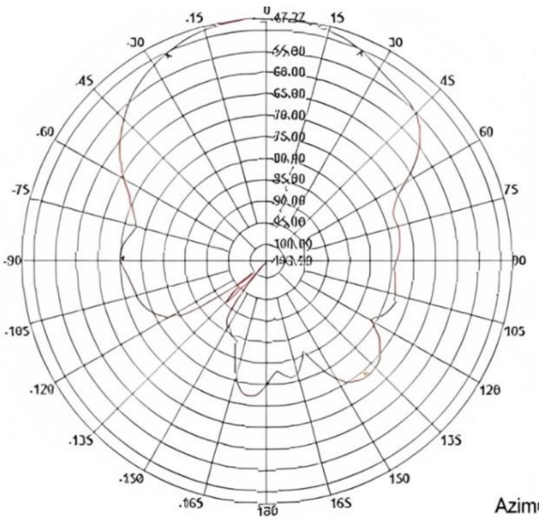

Figure 32. Radiation pattern at 270MHz.

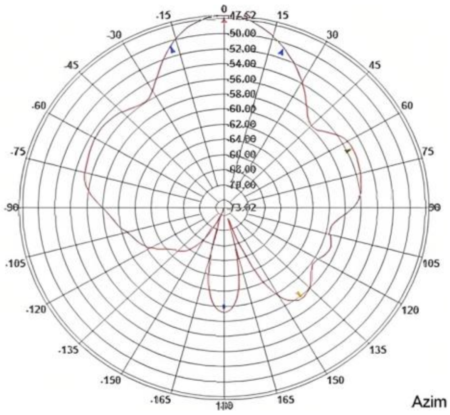

Figure 33. Radiation pattern at 280MHz.

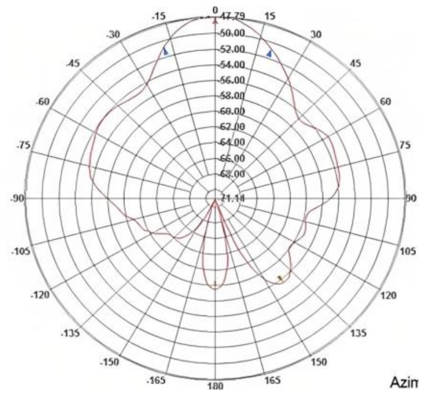

Figure 34. Radiation pattern at 290MHz.

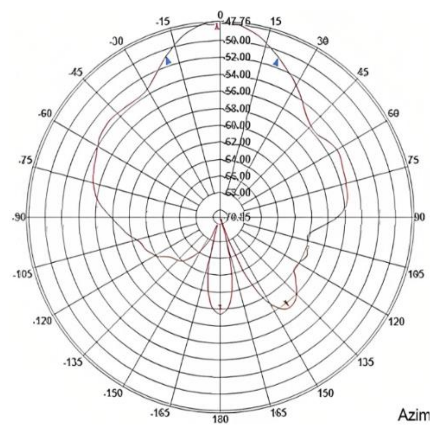

Figure 35. Radiation pattern at 300MHz.

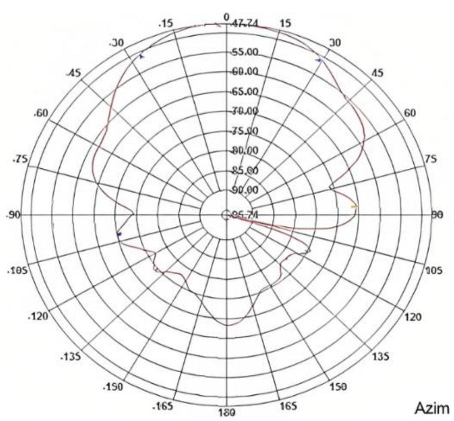

Figure 36. Radiation pattern at 310MHz.

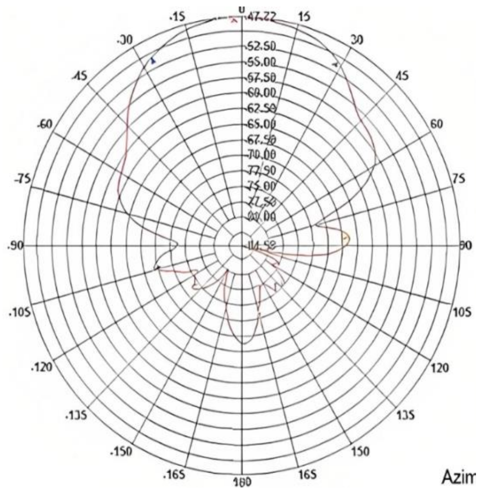

Figure 37. Radiation pattern at 320MHz.

D. Measured VSWR and 3dB Beam Width at Various Resonant Frequencies

The measured VSWR values were taken from Fig. 19, and the measured 3dB beam values were taken from the measured radiation patterns in the horizontal and vertical polarizations, which are provided in Section IV.B and C, respectively.

TABLE IV. VSWR AND 3DB BEAM WIDTH OF FABRICATED ANTENNA IN HP AND VP AT VARIOUS RESONANT FREQUENCIES

Frequency (MHz)	Measured VSWR	Measured 3-dB beam width (deg): 3dB beam width of fabricated antenna in HP	Measured 3-dB beam width (deg): 3dB beam width of fabricated antenna in VP
240	1.99	74.44	94.97
250	1.48	84.63	84.79
260	1.76	116.07	91.52
270	1.71	129.17	81.51
280	2.11	134.07	89.89
290	1.95	149.77	96.7
300	1.80	58.86	93.03
310	2.01	109.05	140.04
320	2.2	102.73	151.35

Table IV shows that the lower VSWR values at the resonant frequencies are, respectively, 1.48 at 250 MHz and 1.80 at 300MHz. For applications involving UHF satellite communication, these values are good and appropriate. The greater 3dB beam width values in the horizontal and vertical polarizations have been noted in Table IV to be 129.17^0 at 270MHz, 149.77^0 at 290MHz, 94.97^0 at 240MHz, and 151.35^0 at 320MHz, respectively. Better and more suited for UHF satellite communication applications are the larger 3dB beam width values.

E. Measured Fabricated Antenna Power, Standard Antenna Power and Standard Antenna Gain at Various Resonant Frequencies

Fabricated antenna power values are obtained at different angles from the measured radiation patterns in horizontal and vertical polarizations, which are presented in sections such as Section IV.B and C.

Table V shows that power values of fabricated antenna in both horizontal and vertical polarizations. The power values are used to calculate the gain of the fabricated antenna. Generally, the power values are measured in dBm's.

TABLE V. FABRICATED ANTENNA POWER IN HP AND VP AT DIFFERENT ANGLES OF Θ, STANDARD ANTENNA POWER AND STANDARD ANTENNA GAIN FOR VARIOUS RESONANT FREQUENCIES

Freq (MHz)	Fabricated antenna power values(dBm) in HP			Fabricated antenna power values(dBm) in VP		
	-45^0	0^0	45^0	-45^0	0^0	45^0
240	-34	-31.65	-38	-33	-31.69	-35
250	-36	-32.24	-36.8	-34.2	-33.2	-36
260	-34	-32.7	-37.8	-36.2	-32.4	-33
270	-34.1	-34.09	-36.5	-34	-33	-36
280	-32.98	-31.97	-35.7	-32.14	-32.34	-35.9
290	-32.64	-32.14	-34	-33.38	-33.20	-36
300	-34.5	-32.42	-33.22	-37	-32.42	-37
310	-38	-33.81	-33.81	-42	-36.73	-40
320	-40.2	-36.38	-36.31	-37.5	-32.50	-37

TABLE VI. STANDARD ANTENNA POWER AND STANDARD ANTENNA GAIN FOR VARIOUS RESONANT FREQUENCIES

Frequency (MHz)	Standard antenna power(dBm)	Standard antenna gain (dBi)
240	-39.24	-3.300
250	-39.35	-4.490
260	-39.67	-4.670
270	-40.59	-4.750
280	-41.5	-4.850
290	-41.6	-4.930
300	-40.89	-5.100
310	-44.11	-5.170
320	-46.99	-5.320

Standard antenna power and standard antenna gain values are equal in both polarizations, as shown in Table VI. The manufactured antenna gain values are computed using the standard antenna power and standard antenna gain values.

F. *Measured Fabricated Antenna Gain in Horizontal and Vertical Polarizations*

Gain is measured in two polarizations, including horizontal and vertical polarizations. Based on the fabricated antenna power, standard antenna power, standard antenna gain, polarization losses, and cable losses, the fabricated antenna gain is computed in this case.

TABLE VII. FABRICATED ANTENNA GAIN AT DIFFERENT ANGLES OF 'Θ' IN HORIZONTAL AND VERTICAL POLARIZATIONS FOR RESONANT FREQUENCIES

Frequency (MHz)	Fabricated antenna gain values (dBi) in HP			Fabricated antenna gain values (dBi) in VP		
	-45^0	0^0	45^0	-45^0	0^0	45^0
240	6.94	9.29	2.94	7.94	9.25	5.44
250	3.86	7.62	3.06	5.65	6.65	3.66
260	6	7.3	2.2	3.8	7.59	6.2
270	6.74	6.75	4.34	6.84	7.76	4.84
280	8.67	9.68	5.95	9.51	9.31	5.75
290	9.03	9.53	7.67	8.29	8.47	5.67
300	6.29	8.37	7.57	3.79	8.37	3.79
310	5.94	10.13	10.13	2.94	8.21	4.94
320	6.47	10.29	10.36	7.61	12.61	8.11

The following equation is used in Table VII to determine the manufactured antenna gain in horizontal and vertical polarizations at various angles for each frequency.

$$\text{Fabricated antenna gain} = \text{Fabricated antenna power minus standard antenna power} + \text{standard antenna gain} + \text{3dB polarization loss} + \text{2dB cable losses} \quad (9)$$

The variables from Table VI are taken into account in Eq. (9), which considers constructed antenna power, standard antenna power, and standard antenna gain. From Table VII, it can be seen that for both horizontal and vertical polarizations, the gain values are maximum at $\theta=0^0$ when compared to -45° and +45°. The greater gain values at 0^0 in horizontal polarization for the resonant frequencies are 9.29dBi at 240MHz and 10.29dBi at 320MHz according to the observation. The higher gain values for -45° and +45° are similarly 6.94dBi at 240MHz, 9.03dBi at 290MHz, 4.34dBi at 270MHz, and 10.36dBi at 320MHz. The higher gain values at 0^0 in vertical polarization are 9.25dBi at 240MHz and 12.61dBi at 320MHz, respectively. The higher gain values are 7.94dBi at 240MHz, 8.29dBi at 290MHz, 6.2dBi at 260MHz, and 8.11dBi at 320MHz, respectively, at -45° and -+45°. The higher gain values that were measured are accurate and appropriate for UHF satellite communication applications.

G. *Measured Axial Ratio*

The radiation patterns in the horizontal and vertical polarizations are provided in B and C of Section IV and the measured constructed antenna power values are used to determine the axial ratio.

TABLE VIII: MEASURED AXIAL RATIO AT DIFFERENT ANGLES OF Θ FOR VARIOUS RESONANT FREQUENCIES

Frequency (MHz)	Measured axial ratio(dB)		
	-45^0	0^0	45^0
240	1	0.04	2.5
250	1.79	0.97	0.6
260	2.2	0.29	4
270	0.1	1.01	0.5
280	0.84	0.37	0.2
290	0.74	1.06	2
300	2.5	0	3.78
310	4	2.92	6.19
320	2.7	3.88	0.69

The following equation is used in Table VIII to get the value of the axial ratio at various angles for each frequency.

$$\text{Axial ratio} = \left| \text{Maximum power of fabricated antenna in HP pattern} - \text{Maximum power of fabricated antenna in VP pattern} \right| \quad (10)$$

The lower axial ratio values at 0^0 for the various resonant frequencies are shown in Table VIII to be 0.04dB at 240MHz and 0dB at 300MHz, respectively. Similar to this, at -45° and +45°, the lower axial ratio values are 0.1dB at 270MHz, 0.74dB at 290MHz, 0.5dB at 270MHz, and 0.69dB at 320MHz, respectively. The reduced axial ratio values that were found are satisfactory and appropriate for UHF satellite communication applications.

V. Results and Discussion

In terms of VSWR, 3dB beam width, gain, and axial ratio at various resonant frequencies, all the simulated and measured findings are compared. The fabrication of the antenna for use in UHF satellite communication applications is validated through the comparison of simulated and measured findings.

The improved measured VSWR values are achieved when compared to the generated VSWR values, and these values are extremely well matched, as can be shown in Table IX. As compared to the simulated 3dB beam width values, the horizontal and vertical polarization 3dB beam width values are known as the better measured 3dB beam width values.

TABLE IX. Comparison of Simulated and Measured Results in Terms of VSWR and 3dB Beam Width for Various Resonant Frequencies

Fr equenc y (MHz)	Simula ted VSWR	Meas ured VS WR	Simula ted beam width	Measured beam width in HP	Measured beam width in VP
240	2.350	1.99	84.3	74.44	94.97
250	1.776	1.48	88.1	84.63	84.79
260	1.396	1.76	91.8	116.07	91.52
270	1.461	1.71	95.3	129.17	81.51
280	1.737	2.11	89.7	134.07	89.89
290	1.769	1.95	102.8	149.77	96.7
300	1.865	1.80	106.7	58.86	93.03
310	1.980	2.01	110.8	109.05	140.04
320	2.063	2.2	114.9	102.73	151.35

Table IX shows that comparison of simulated and measured VSWR values at all receiving and transmitting frequencies.

TABLE X. Comparison of Simulated and Measured Gain in Horizontal and Vertical Polarizations at ϴ=-450 SG-Simulated Gain, MGHP-Measured Gain in Horizontal Polarization, MGVP-Measured Gain in Vertical Polarization

Frequency (MHz)	Simulated gain	Measured gain in HP	Measured gain in VP
	-45^0	-45^0	-45^0
240	0.606	6.94	7.94
250	0.756	3.86	5.65
260	1.425	6	3.8
270	2.146	6.74	6.84
280	2.733	8.67	9.51
290	3.320	9.03	8.29
300	3.026	6.29	3.79
310	3.195	5.94	2.94
320	3.415	6.47	7.61

TABLE XI: Comparison of Simulated and Measured Gain in Horizontal and Vertical Polarizations At $\theta = 0^0$ and 45^0

Freq (MHz)	SG	MGHP	MGVP	SG	MGHP	MGVP
	0^0	0^0	0^0	45^0	45^0	45^0
240	6.3	9.29	9.2	2.94	2.94	5.44
250	6.6	7.62	6.6	3.40	3.06	3.66
260	6.8	7.3	7.5	3.52	2.2	6.2
270	6.6	6.75	7.7	3.40	4.34	4.84
280	6.4	9.68	9.3	3.38	5.95	5.75
290	5.9	9.53	8.4	3.61	7.67	5.67
300	5.6	8.37	8.3	3.30	7.57	3.79
310	5.2	10.1	8.2	3.39	10.1	4.94
320	4.7	10.2	12.	3.48	10.3	8.11

It is evident from Tables X and XI that the measured gain in horizontal and vertical polarizations is superior to the calculated gain at the various angles of (-45^0, 0^0, and 45^0).

Table XII shows that at the various angles of, the measured axial ratio values are more accurate than the simulated axial ratio values (-45^0, 0^0, and 45^0).

TABLE XII. Comparison of Simulated and Measured Axial Ratio at Different Angles of ϴ for Various Resonant Frequencies
SAR-Simulated axial ratio and MAR-Measured axial ratio

Freq (MHz)	SAR	MAR	SAR	MAR	SAR	MAR
	-45^0	-45^0	0^0	0^0	45^0	45^0
240	3.596	1	2.014	0.04	3.624	2.5
250	2.586	1.79	2.188	0.97	2.622	0.6
260	2.069	2.2	2.835	0.29	2.125	4
270	2.182	0.1	2.912	1.01	2.193	0.5
280	1.303	0.84	2.044	0.37	2.044	0.2
290	0.418	0.74	1.208	1.06	0.430	2
300	1.601	2.5	1.505	0	1.586	3.78
310	1.492	4	1.240	2.92	1.470	6.19
320	1.606	2.7	1.950	3.88	1.585	0.69

VI. Conclusion

A double-wire helical antenna was created using the butterfly approach for use in ultra-high frequency (UHF) satellite communication applications in the 240MHz to 270MHz and 290MHz to 320MHz frequency ranges, respectively. Four crucial factors, including the 3dB beamwidth, gain, axial ratio, and VSWR, are examined once this antenna is designed in modelling software. It was approved for construction of the intended antenna after research. The same four crucial parameters were tested after construction, and their values are compared to those predicted. From the measured results, the lower VSWR values at the resonant frequencies are 1.48 at 250MHz and 1.80 at 300MHz, respectively. The greater 3dB beam width values in the horizontal and vertical polarizations have been noted to be 129.17^0 at 270MHz, 149.77^0 at 290MHz, 94.97^0 at 240MHz, and 151.35^0 at 320MHz, respectively. The greater gain values at 0^0 in horizontal polarization for the resonant frequencies are 9.29dBi at 240MHz and 10.29dBi at 320MHz.The higher gain values at 0^0 in vertical polarization are 9.25dBi at 240MHz and 12.61dBi at 320MHz, respectively. The lower axial ratio values at 0^0 for the various resonant frequencies are to be 0.04dB at 240MHz and 0dB at 300MHz, respectively. Similar to this, at -45° and +45°, the lower axial ratio values are 0.1dB at 270MHz, 0.74dB at 290MHz, 0.5dB at 270MHz, and 0.69dB at 320MHz, respectively. All of the values are in respectable agreement after comparison. In the end, a built-in antenna will be more appropriate for applications involving ultra-high frequency (UHF) satellite communication.

Conflict of Interest

We are declaring that there are no conflicts between the corresponding author and co-authors.

AUTHOR'S CONTRIBUTIONS

The first two authors have collected the data and designed the antenna in the simulation software to get simulation results. The third and fourth authors have analyzed the simulation results and also fabricated the designed antenna. The fifth author has taken the measurement results for a fabricated antenna. Finally, all the authors have compared the simulation and measured results for the validation of the designed antenna and approved the final version of the paper.

REFERENCES

[1] W. Jiang, "Software defined satellite networks: A survey," *Digital Communications and Networks*, 2023.

[2] F. A. Dicandia, N. J. G. Fonseca, M. Bacco *et al.*, "Space-air-ground integrated 6G wireless communication networks: A Review of antenna technologies and application scenarios," *Sensors*22, no. 9, p. 3136, 2022.

[3] G. He, X. Gao, L. Sun *et al.*, "A Review of multibeam phased array antennas as LEO satellite constellation ground station," *IEEE Access*, 2021, vol. 9, pp. 147142-147154.

[4] C. L. Chen, "A dual-band circularly polarized shared-aperture antenna for 1U CubeSat applications," *IEEE Transactions on Antennas and Propagation*, vol. 70, Issue 5, pp. 3818–3823, DOI:10.1109/TAP.2021.312537, May 2022.

[5] S. Abulgasem, F. Tubbal Raad, *et al.*, "Antenna designs for CubeSats: A review," *IEEE Access*, vol. 9, pp. 45289–45324, March 2021, DOI: 10.1109/ACCESS.2021.3066632.

[6] X. Zhang *et al.*, "Compact UHF/VHF monopole antennas for CubeSats applications," *IEEE Access*, July 2020, vol. 8, pp. 133360–133366, DOI: 10.1109/ACCESS.2020.3008540.

[7] M. T. Islam, S. Kibria, and M. G. Cho, "BIRDS-1 CubeSat Constellation Using Compact UHF Patch Antenna," *IEEE Access*, vol. 6, pp. 54282–54294, September 2018.

[8] G. C. Huang and M. F. Iskander, "A low-profile UHF SATCOM Antenna," *IEEE Transactions on Antennas and Propagation*, vol. 66, Issue 9, pp. 4890–4894, September 2018.

[9] S. W. Liao and Q. Xue, "Miniaturized VHF/UHF dual-band circularly polarized four-element sequential-rotation array antenna based on alternately overlapped bent radiation-coupled dual-l antenna elements," *IEEE Transactions on Antennas and Propagation*, vol. 66, Issue 9, pp. 4924–929, September 2018, DOI: 10.1109/TAP.2018.2851668.

[10] L. Vincent, C. W. Trueman, and S. Gleason, "Design and implementation of IPLEXER and a Dual-Band VHF/UHF Antenna for nanosatellites," *IEEE Antennas and Wireless Propagation Letters*, vol. 12, pp. 1098–1101, September 2013, DOI: 10.1109/AWP.2013.220454.

[11] J. Costantine, Y. Tawk, I. Maqueda, M. Sakovsy, and G. Olson, "UHF deployable helical antennas for CubeSats," *IEEE Transactions on Antennas and Propagation*, vol. 64, Issue 9, pp. 3752–3759, Sept. 2016, DOI:10.1109/TAP. 2016.2308.

[12] M. Hosseini, M. Hakkak, and P. Rezaei, "Design of a dual-band quadrifilar helix antenna," *IEEE Antennas and Wireless Propagation Letters*, vol. 4, pp. 39–42, February 2005, DOI: 10.1109/LAWP.2005.844142.

[13] C. J. Deng *et al.*, "A circularly polarized pattern diversity antenna for hemispherical coverage," *IEEE Transactions on Antennas and Propagation*, October 2014, vol. 62, Issue 10, pp. 5365–5369, DOI: 10.1109/TAP.2014.2342763.

[14] I. Tzanidis, C.-C. Chen, and J. L.Volakis, "Low profile spiral on a thin ferrite ground plane for 220–500 MHz operation," *IEEE Transactions on Antennas and Propagation*, November 2010, Volume 58, Issue 11, pp. 3715–3720, DOI: 10.1109/TAP.2010.2071337.

[15] J. D Kraus, R. T. Mishawaka, and A. S. Khan, *Antennas for All application*, The Mc Graw Hill companies (Third edition) 2006.

[16] R. K. Stilwell, *Satellite Applications of the Bifilar Helix Antenna*, Johns Hopkins, APL Technical Digest, vol. 12, no. 1, 1991.

[17] T. Pratt and C. Bostian, *Satellite Communications*, 2nd edition, John Wiley &Sons, 2003.

[18] S. W. Yang, S. H. Tan, and J. Xia, "FDTD design of bifilar and Quadrifilar truncated spherical helical antennas," *Microwave and Optical Technology Letters*, vol. 30, no. 4, 2001.

[19] J. Yamauchi, H. Nakano, and H. Mimaki, "Backfire bifilar helical antenna with tapered feed end," in *Proc. 1981 Antennas and Propagation Society International Symposium*, Los Angeles, CA, USA, 1981, pp. 683-686.

[20] X.-Y. QU, and W.-H. Zong, "The design of shaped beam bifilar helix antenna with conical pattern," *LNICST72*, pp. 287–292, 2012.

[21] M. Amin, J. Yousaf, and S. Iqbal, "Single feed circularly polarized Omnidirectional bifilar helix antennas with wide axial ratio beam width," *IET, Microwave Antenna Propagation*, vol. 7, Issue:10, pp. 825-830, 2013.

[22] H. Nakano, "Improvement in front to a Back ratio of a Bifilar Backfire helix by a Flared open-end," *IEEE Transactions on Antennas and propagation*, vol. 41, No.11, November 1993.

[23] Y. Konishi, M. Ohtsuka, M. Matsunaga, and T. Katagi, "A linear array antenna using bifilar helical elements for mobile satellite communications," in *Proc. IEEE Antennas and Propagation Society International Symposium and URSI National Radio Science Meeting*, Seattle, WA, USA, 1994, pp. 1020-1023, vol. 2.

[24] X. L. Liu, S. Yao, B. S. Cook, M. M. Tentzeris, and S. V. Georgeakopoulos, "An origami reconfigurable axial-mode bifilar helical antenna," *IEEE Transactions on Antennas and Propagation*, vol. 63, no. 12, December 2015.